# Photoinduced Electron Transfer in Supramolecular Ruthenium-Porphyrin Assemblies.

*Diego Rota Martir,[a] Mattia Averardi, Daniel Escudero,[b] Denis Jacquemin[b,c] and Eli Zysman-Colman[a]**

[a] Organic Semiconductor Centre, EaStCHEM School of Chemistry, University of St Andrews, St Andrews, Fife, KY16 9ST, UK, Fax: +44-1334 463808; Tel: +44-1334 463826; E-mail: eli.zysman-colman@st-andrews.ac.uk;
URL: http://www.zysman-colman.com
[b] CEISAM UMR CNRS 6230, Université de Nantes, 2 rue de la Houssinière, BP 92208, 44322 Nantes Cedex 3, France
[c] Institut Universitaire de France, 1, rue Descartes, 75005 Paris Cedex 5, France

## SUPPORTING INFORMATION

## Table of Contents:

# Experimental section.

*General Synthetic Procedures*. Commercial chemicals were used as supplied. All reactions were performed using standard Schlenk techniques under inert ($N_2$) atmosphere with reagent-grade solvents. Flash column chromatography was performed using silica gel (Silia-P from Silicycle, 60 Å, 40-63 μm). Analytical thin layer chromatography (TLC) was performed with silica plates with aluminum backings (250 μm with indicator F-254). Compounds were visualized under UV light. $^{1}H$,$^{13}C$ and$^{19}F$ solution-phase NMR spectra were recorded on a BrukerAvance spectrometer operating at 11.7 T (Larmor frequencies of 500, 126 and 471 MHz, respectively). The following abbreviations have been used for multiplicity assignments: “s” for singlet, “d” for doublet, “t” for triplet, “m” for multiplet and “br” for broad. The solvent was $CD_2Cl_2$. Melting points (Mps) were recorded using open-ended capillaries on an Electrothermal melting point apparatus and are uncorrected. High-resolution mass spectra were recorded at the EPSRC UK National Mass Spectrometry Facility at Swansea University on a quadrupole time-of-flight (ESI-Q-TOF), modelABSciex 5600 Triple TOF in positive electrospray ionization mode and spectra were recorded using sodium formate solution as the calibrant.

# Synthesis of complexes 1 and 2.

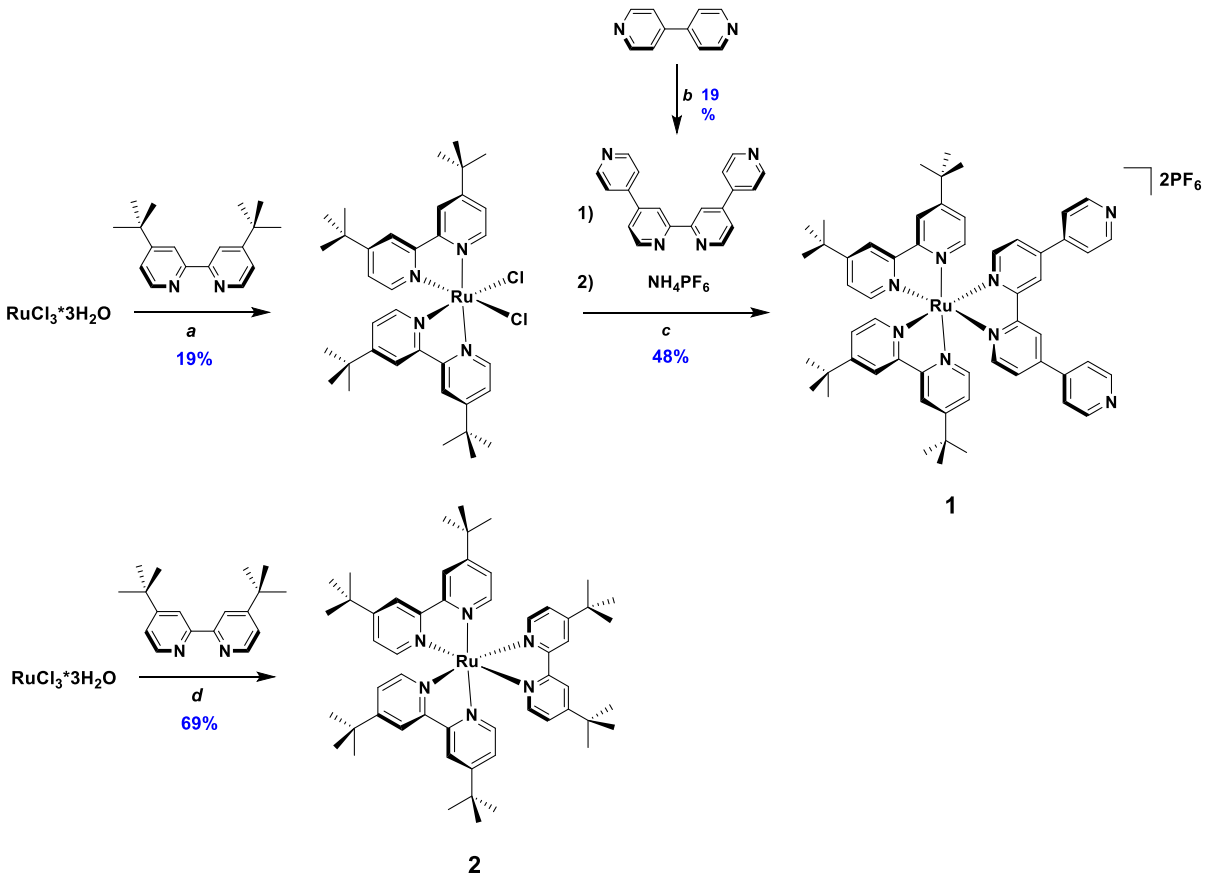


Scheme **S1**. Synthesis of complexes [Ru(dtBubpy)$_2$(qpy)]2PF$_6$, **1** and [Ru(dtBubpy)$_3$]2PF$_6$, **2**. Reagents and conditions. [a] 4.0 equiv. LiCl, $N_2$, dark, DMF, 140 °C, 6 h; [b] DMF, 10 mol% Pd/C, 165°C, 48h, [c] i. ethylene glycol, 160 °C, 1 h, $N_2$; ii. Excess solid $NH_4PF_6$; [d] ethylene glycol, 160 °C, 1 h, $N_2$.

**Synthesis of bis-(4,4'-di-tert-butyl-2,2'-bipyridine)-dichloro ruthenium(II), Ru(dtBubpy)$_2$Cl$_2$.**

The synthesis of this complex is by a modified method to that previously reported.[1]

$RuCl_3$*x$H_2O$ (207 mg, 0.792 mmol, 1 equiv.), 4,4′-Di-*tert*-butyl-2,2′-dipyridyl (400 mg, 1.490 mmol, 2 eq) and LiCl (126.3 mg, 2.98 mmol, 4 equiv.) were added to a round bottom flask containing 15 mL of DMF. The mixture was refluxed under nitrogen atmosphere and in absence of light for 6 hours and then cooled to room temperature. Most of the solvent was removed by evaporation under reduced pressure, diethyl ether was added and the resultant solution was cooled at -25°C overnight. Filtering the resulting mixture yielded a red to red-violet filtrate and a nearly black microcrystalline product. The solid was washed well with several portions of cold water, followed by several portions of diethyl ether. **Yeld** 19.0 %. **$^1$H NMR (400 MHz, DMSO-$d_6$) δ (ppm)**: 9.83 (d, *J* = 2.0 Hz, 2H), 8.63 (d, *J* = 2.0 Hz, 2H), 8.47 (d, *J* = 2.1 Hz, 2H), 7.77 (dd, *J* = 6.1, 2.1 Hz, 2H), 7.38 (d, *J* = 6.2 Hz, 2H), 7.14 (dd, *J* = 6.2, 2.1 Hz, 2H), 1.51 (s, 18H), 1.28 (s, 18H).
The characterisation matches that reported.[2]

**Synthesis of 4,4':2',2'':4'',4'''-quaterpyridine (qpy).**

The synthesis of this ligand followed that previously reported.[3]
4,4'-Bipyridine (5.0 g, 0.032 mol), Pd/C (0.70 g, 10% weight Pd) and DMF (50 mL) were added to a dry round bottomed flask, and the reaction mixture was sonicated and oxygenated by bubbling air through the solution. The mixture was refluxed at 165˚ for 48 h, cooled to room temperature and the solvent was removed using high vacuum rotary evaporator. The crude product was dissolved in $CHCl_3$ (50 mL) and the catalyst was filtered. A bright yellow solution was obtained and $CHCl_3$ was distilled under vacuum to obtain a brown solid (7.5 g). The crude was purified by flash chromatography (5% methanol / dichloromethane). To give 0.9 g as pure compound as a white solid. **Yield:** 15%. **$R_f$:** 0.40 (5% MeOH/DCM on silica). **$^1$H NMR (500 MHz, $CDCl_3$) δ (ppm):** 8.86 (d, *J* = 5.4 Hz, 2H), 8.82 – 8.79 (m, 6H), 7.71 (d, *J* = 5.1 Hz, 4H), 7.64 (d, *J* = 5.5, 2H). **$^{13}$C NMR (126 MHz, $CDCl_3$) δ (ppm):** 156.6, 150.7, 150.1, 146.7, 145.6, 121.7, 121.5, 119.1. The characterization matches that reported.[3]

**Synthesis of bis-(4,4'-di-tert-butyl-2,2'-bipyridine)ruthenium(II) 4,4':2',2'':4'',4''' quaterpyridine hexafluorophosphate [Ru(dtBubpy)$_2$(qpy)](PF$_6$)$_2$.**

The synthesis of this complex is by a modified method to that previously reported.[4]
Ru(dtBubpy)$_2$Cl$_2$ (91 mg, 0.129 mmol, 1 equiv.) and 4,4':2',2'':4'',4'''-quaterpyridine (40 mg, 0.129 mmol, 1 equiv.) were added to a round bottom flask containing 13 mL of ethylene glycol. The mixture was refluxed

under nitrogen atmosphere for 1 hour and then cooled to room temperature and filtered. A saturated, aqueous $NH_4PF_6$ solution was added to the filtrate and a red precipitate was filtered off and washed with water and diethyl ether. The crude product was purified by silica flash chromatography (silica, acetone : acetonitrile 1:1 with $NH_4PF6$ 0.3 M ); after an initial orange fraction was removed, the major red fraction was evaporated to dryness, washed with water and dried to yield an orange solid. **Yeld**: 47.5%. **Rf**: 0.4 (acetone/acetonitrile, 1 : 1 with $NH_4PF6$ 0.3 M on silica). **$^1$H NMR (500 MHz, $CD_2Cl_2$) δ (ppm)**: 8.86 (d, *J* = 1.9 Hz, 2H, $H_a$), 8.71 (m, 4H, $H_b$), 8.31 (d, *J* = 2.0 Hz, 2H, $H_c$), 8.29 (d, *J* = 2.0 Hz, 2H, $H_d$), 8.05 (m, 4H, $H_e$), 7.89 (d, *J* = 6.0 Hz, 2H, $H_f$), 7.77 (dd, *J* = 6.0, 1.9 Hz, 2H, $H_g$), 7.71 (d, *J* = 6.1 Hz, 1H, $H_h$), 7.62 (d, *J* = 6.0 Hz, 2H, $H_i$), 7.48 (m, 4H, $H_j$), 1.43 (s, 9H, $H_k$), 1.39 (s, 9H, $H_l$).**$^{13}$C NMR (126 MHz, $CD_2Cl_2$) δ (ppm)**: 163.3, 158.1, 156.8, 156.6, 152.5, 151.4, 150.9, 147.8, 147.7, 147.4, 145.7, 126.2, 125.9, 123.7, 123.7, 122.6, 121.2, 121.2, 121.2, 121.2, 35.9, 35.9, 30.4, 30.4, 30.4, 30.3, 30.3, 30.3. **FT NSI+ MS**: [M − 2PF6] 2+ Calculated (C56H62N8Ru): 474.2070; Found: 474.2060.

**Synthesis of tris-(4,4'-di-tert-butyl-2,2'-bipyridine)ruthenium(II) hexafluorophosphate, $[Ru(dtBubpy)_3](PF_6)_2$.**

The synthesis of this complex is by a modified method to that previously reported.[5]

$RuCl_3$*x$H_2O$ (55 mg, 0.210 mmol, 1 equiv.) and 4,4′-Di-*tert*-butyl-2,2′-dipyridyl (198 mg, 0.736 mmol, 3.5 equiv.) were added to a round bottom flask containing 25 mL of ethylene glycol. The mixture was refluxed under nitrogen atmosphere for 1 hour and then cooled to room temperature. A saturated, aqueous $NH_4PF_6$ solution was added to the filtrate and an orange precipitate was filtered off and washed with water, diethyl ether and hexane. **Yeld**: 68.7%. **$^1$H NMR (400 MHz, $CD_2Cl_2$) δ (ppm)**: 8.25 (d, *J* = 2.0 Hz, 6H), 7.57 (d, *J* = 6.0 Hz, 6H), 7.45 (dd, *J* = 6.0, 2.0 Hz, 6H), 1.42 (s, 54H). **FT NSI+ MS**: [M − 2PF6] 2+ Calculated (C54H72N6Ru): 453.2429; Found: 453.2415. The characterisation matches that reported.[6]

**Synthesis of zinc tetraphenylphorphyrin, (ZnTPP).**

The synthesis of ZnTPP followed that previously reported.[3]

Tetraphenylporphyrin TPP (0.1 g, 0.162 mmol) was dissolved in 25 mL of chloroform. The solution was purged with nitrogen for 10 min. Zinc acetate (0.073 g, 0.33 mmol) was dissolved in ~ 5 mL methanol and then added to the porphyrin solution. The mixture was stirred under nitrogen overnight at room temperature.

All solvents were removed under reduced pressure leaving, a purple solid. The solid was dissolved in DCM and washed with 3 × 20 mL portions of 5 % w/v aqueous sodium bicarbonate, followed by 3 × 20 mL portions of water. The organic layer dried over $MgSO_4$ and the solvent was removed under reduced pressure. The zinc porphyrin was purified by flash column chromatography on a silica gel using 100% chloroform as the eluent. **Yield:** 90%. **$R_f$:** 0.65 ($CHCl_3$). **$^1$H NMR (500 MHz, $CDCl_3$) δ(ppm)**:8.88 (s, 8H), 8.15 (dd, *J* = 7.4, 1.6 Hz, 8H), 7.69 (m, 12H). **$^{13}$C NMR (126 MHz, $CDCl_3$) δ(ppm)**: 150.2, 142.8, 134.4, 131.9, 127.5, 126.6, 121.1. FT NSI+ MS: [M + H] + Calculated (C44H29N4Zn): 677.1684; Found: 677.1683. The characterization matches that reported.[3]

*General procedure for the synthesis of **1a** and **1b**.* The synthesis of the assemblies **1a** and **1b** followed that previously reported.[3] In a dry 2 mL vial, complex **1** and ZnTPP (1 or 2 equiv.) were dissolved in $CD_2Cl_2$ (1 mL) to give a concentration of the iridium complex of approximately 0.05 M. The solution was sonicated for few seconds and subsequently transferred to an NMR tube for characterization.

*Photophysical measurements*. All samples were prepared in HPLC grade dichloromethane with varying concentrations in the order of $10^{-3}$ – $10^{-5}$ M. Absorption spectra were recorded at room temperature using a Shimadzu UV-1800 double beam spectrophotometer. Molar absorptivity determination was verified by linear least-squares fit of values obtained from at least four independent solutions at varying concentrations with absorbance ranging from $6.05 \times 10^{-5}$ to $2.07\times 10^{-5}$M.

The sample solutions for the emission spectra were prepared in HPLC-grade DCM and degassed *via* three freeze-pump-thaw cycles using a quartz cuvette designed in-house. Steady-state emission and excitation spectra and time-resolved emission spectra were recorded at 298 K using an Edinburgh Instruments F980. All samples for steady-state measurements were excited at 420, 500 and 550 nm, while samples for time-resolved measurements were excited at 378 nm. Emission quantum yields were determined using the optically dilute method.[7] A stock solution with absorbance of *ca*. 0.5 was prepared and then four dilutions were prepared with dilution factors between 2 and 20 to obtain solutions with absorbances of *ca*. 0.095 0.065, 0.05 and 0.018, respectively. The Beer-Lambert law was found to be linear at the concentrations of

these solutions. The emission spectra were then measured after the solutions were rigorously degassed *via* three freeze-pump-thaw cycles prior to spectrum acquisition. For each sample, linearity between absorption and emission intensity was verified through linear regression analysis and additional measurements were acquired until the Pearson regression factor ($R^2$) for the linear fit of the data set surpassed 0.9. Individual relative quantum yield values were calculated for each solution and the values reported represent the slope value. The equation $\Phi_s = \Phi_r(A_r/A_s)(I_s/I_r)(n_s/n_r)$ was used to calculate the relative quantum yield of each of the sample, where $\Phi_r$ is the absolute quantum yield of the reference, $n$ is the refractive index of the solvent, $A$ is the absorbance at the excitation wavelength, and $I$ is the integrated area under the corrected emission curve. The subscripts s and r refer to the sample and reference, respectively. A solution $[Ru(bpy)_3]Cl_2$ in aerated $H_2O$ at 298 K ($\Phi_r = 4\%$) were used as external references.[8]

*Electrochemistry measurements*. Cyclic voltammetry measurements were performed on an Electrochemical Analyzer potentiostat model 600D from CH Instruments. Solutions for cyclic voltammetry were prepared in DCM and degassed with DCM-saturated nitrogen by bubbling for about 10 min prior to scanning. Tetra(*n*-butyl)ammonium hexafluorophosphate ($TBAPF_6$; *ca*. 0.1 M in ACN) was used as the supporting electrolyte. A $Ag/Ag^+$ electrode (silver wire in a solution of 0.1 M KCl in $H_2O$) was used as the pseudoreference electrode; a Pt electrode was used for the working electrode and a Pt electrode was used as the counter electrode. The redox potentials are reported relative to a saturated calomel electrode (SCE) electrode with a ferrocene/ferrocenium ($Fc/Fc^+$) redox couple as an internal reference (0.46 V *vs*. SCE).[9]

# Characterization of complexes.

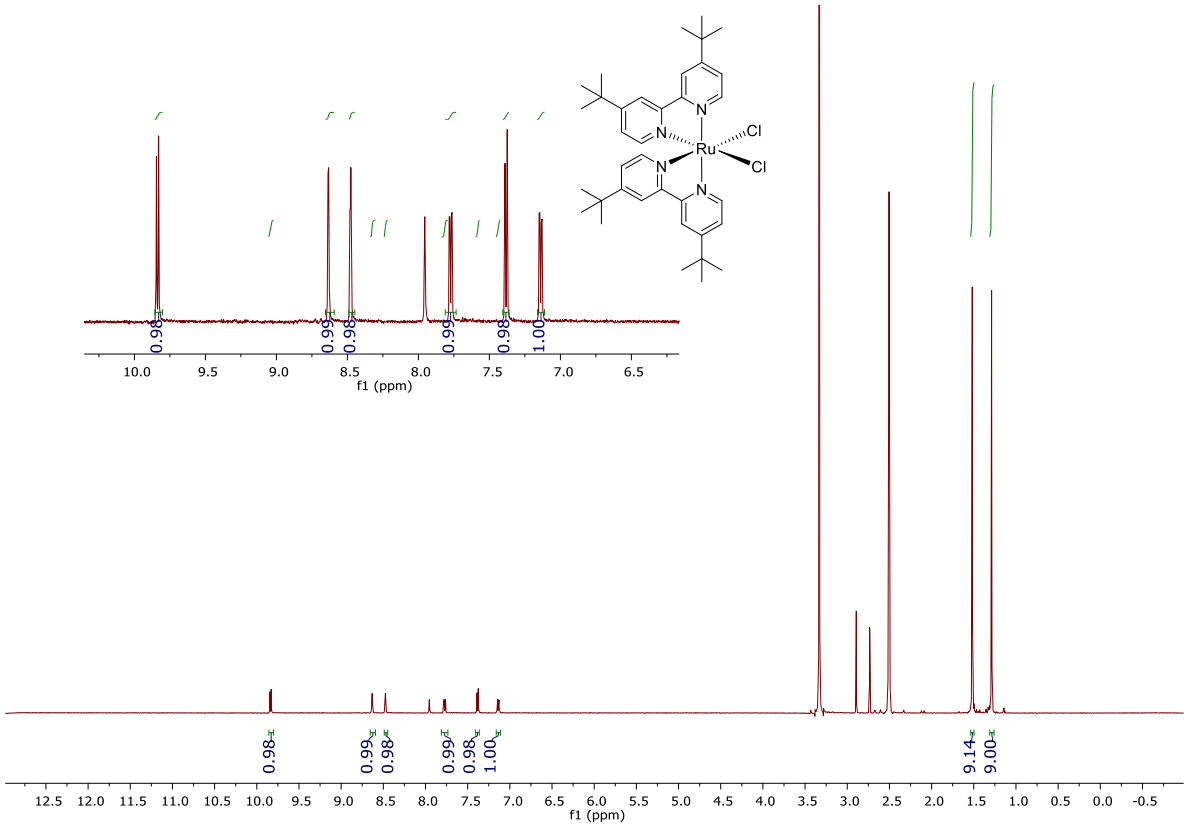


Figure **S1**. $^{1}$H NMR spectrum (400 MHz, DMSO-$d_6$) of Ru(dtBubpy)$_2$Cl$_2$.

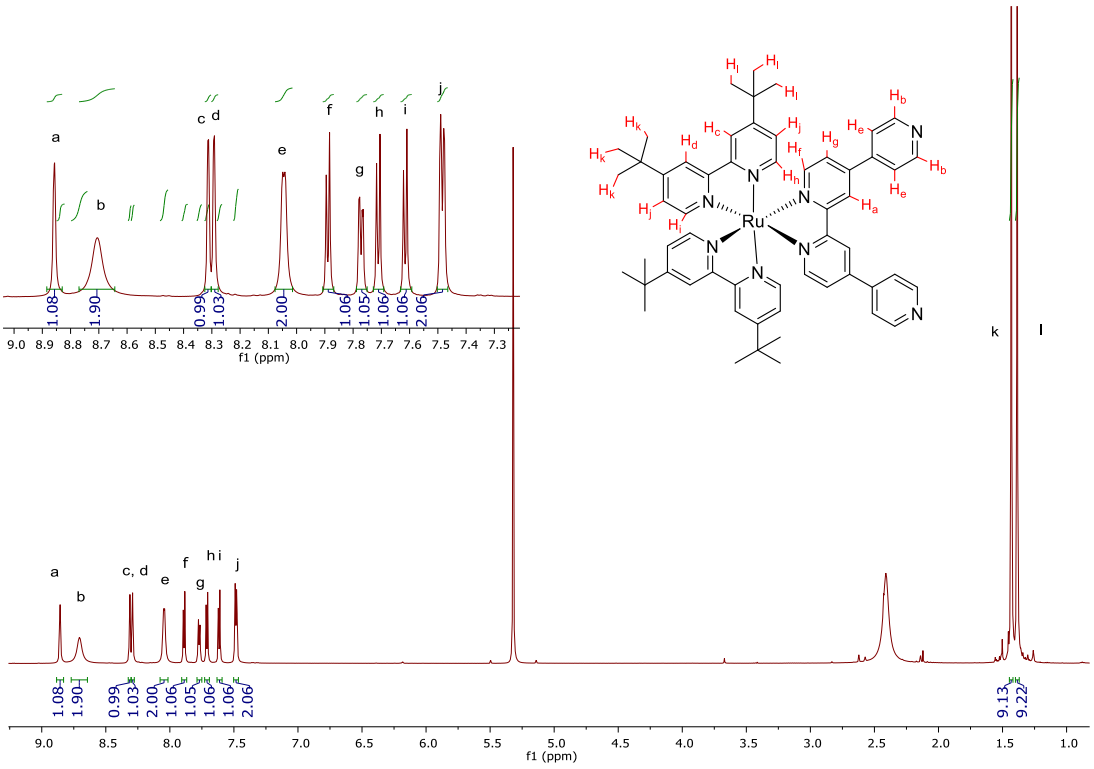


Figure **S2**. $^{1}$H NMR spectrum (400 MHz, $CD_2Cl_2$) of [Ru(dtBubpy)$_2$(qpy)](PF$_6$)$_2$, **1**.

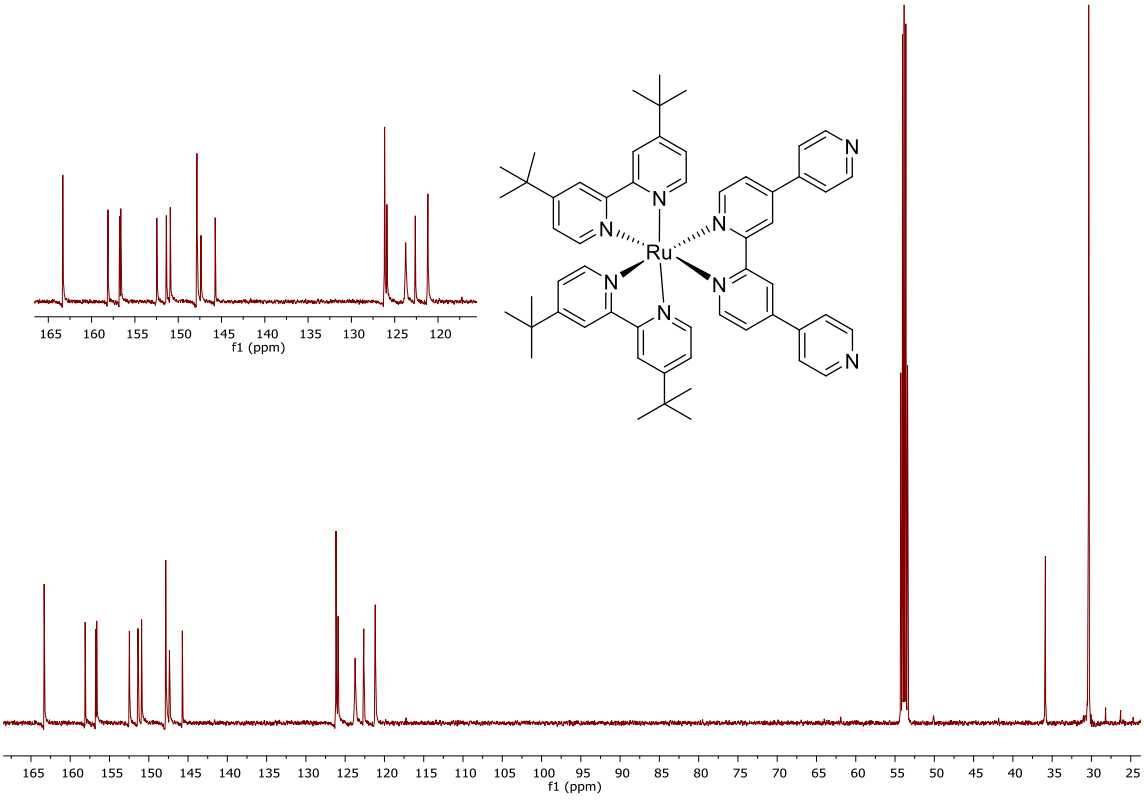


Figure **S3**. $^{13}C$ NMR spectrum (126 MHz, $CD_2Cl_2$) $[Ru(dtBubpy)_2(qpy)](PF_6)_2$, **1**.

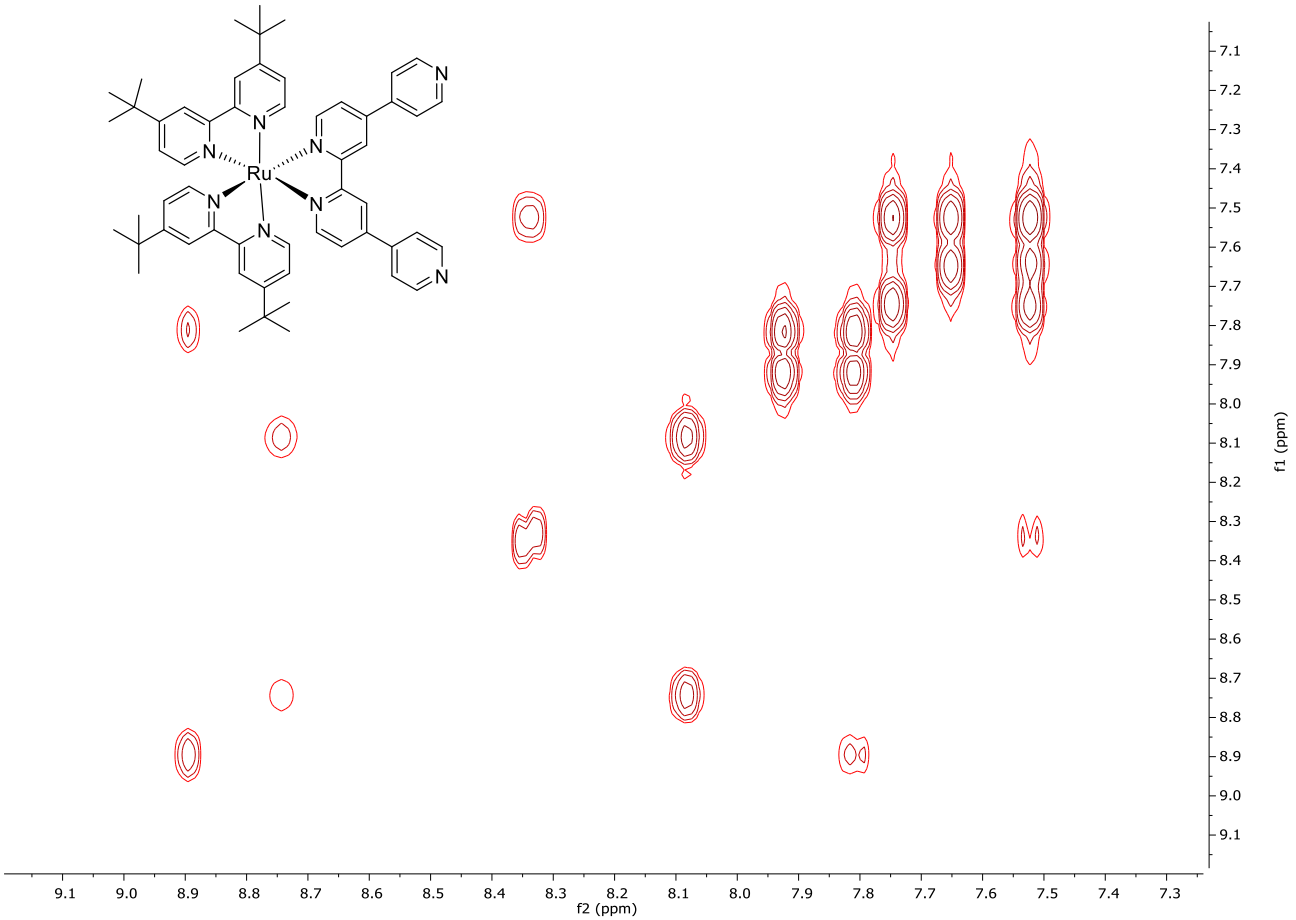


Figure **S4**. 2D-COSY NMR spectrum (500 MHz, $CD_2Cl_2$) $[Ru(dtBubpy)_2(qpy)](PF_6)_2$, **1**.

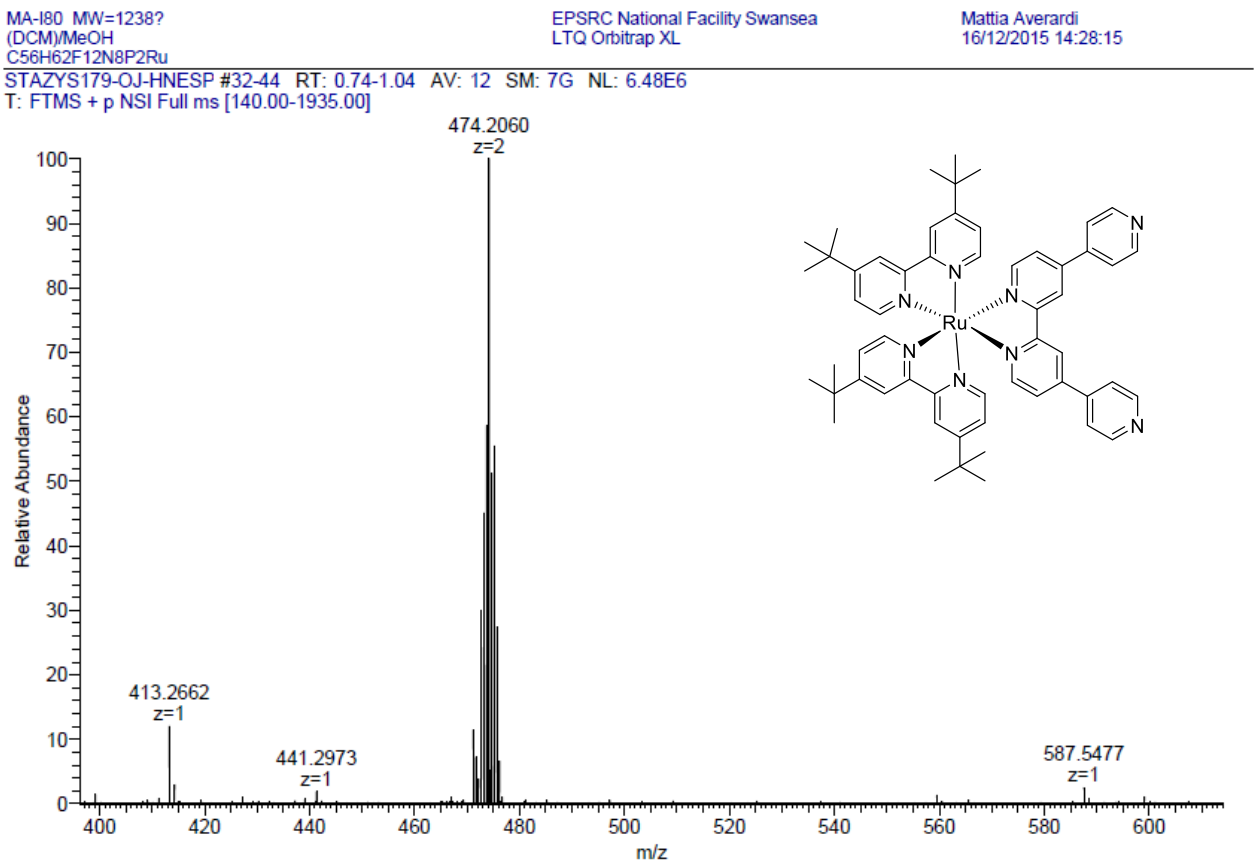


Figure **S5**. HR-MS spectrum of $[Ru(dtBubpy)_2(qpy)](PF_6)_2$, **1**.

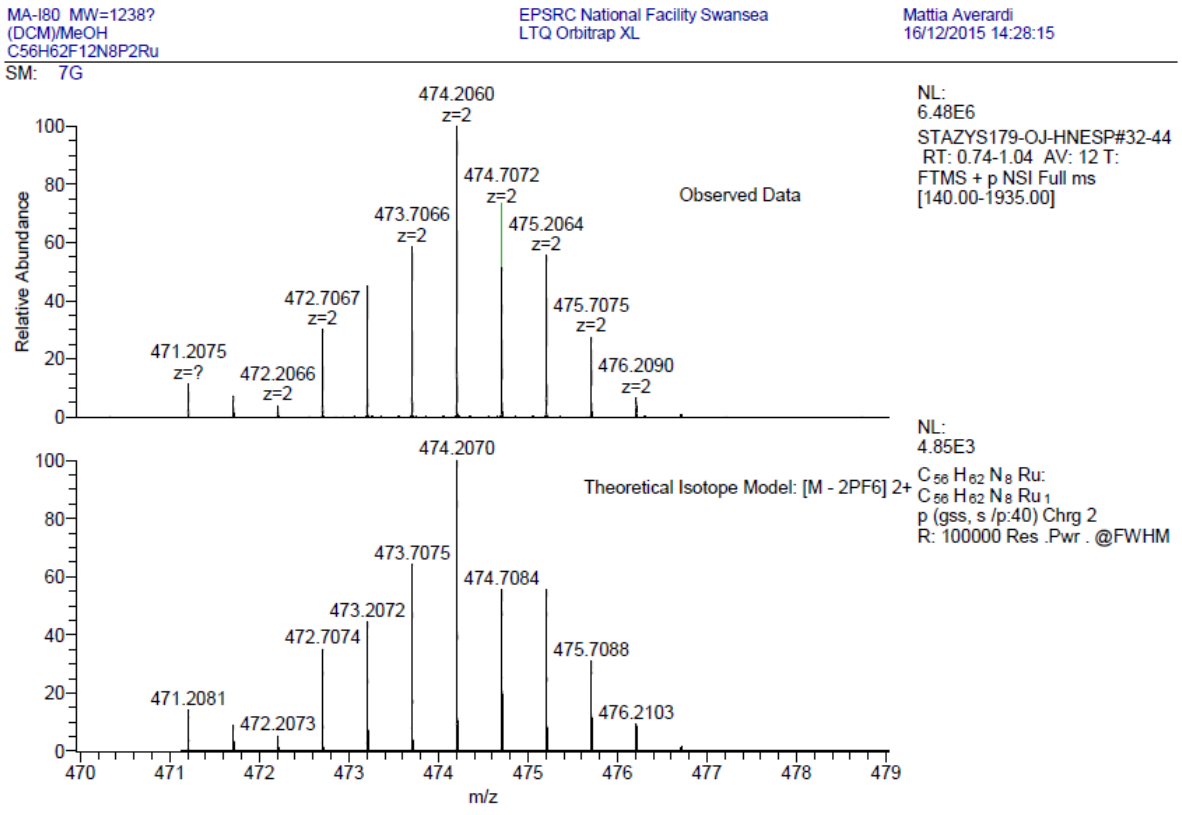


Figure **S6**. Molecular ion of HR-MS spectrum of $[Ru(dtBubpy)_2(qpy)](PF_6)_2$, **1**.

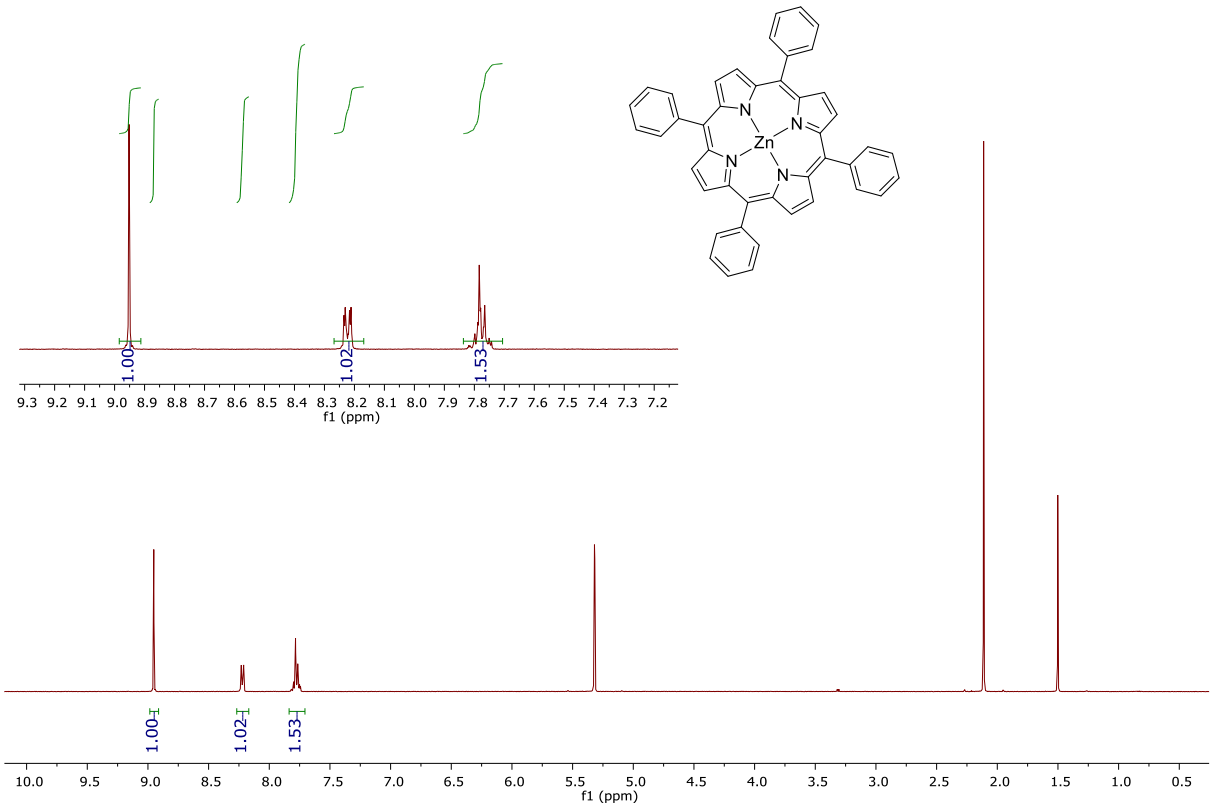


Figure **S7**. $^{1}$H NMR spectrum (400 MHz, $CD_2Cl_2$) of ZnTPP.

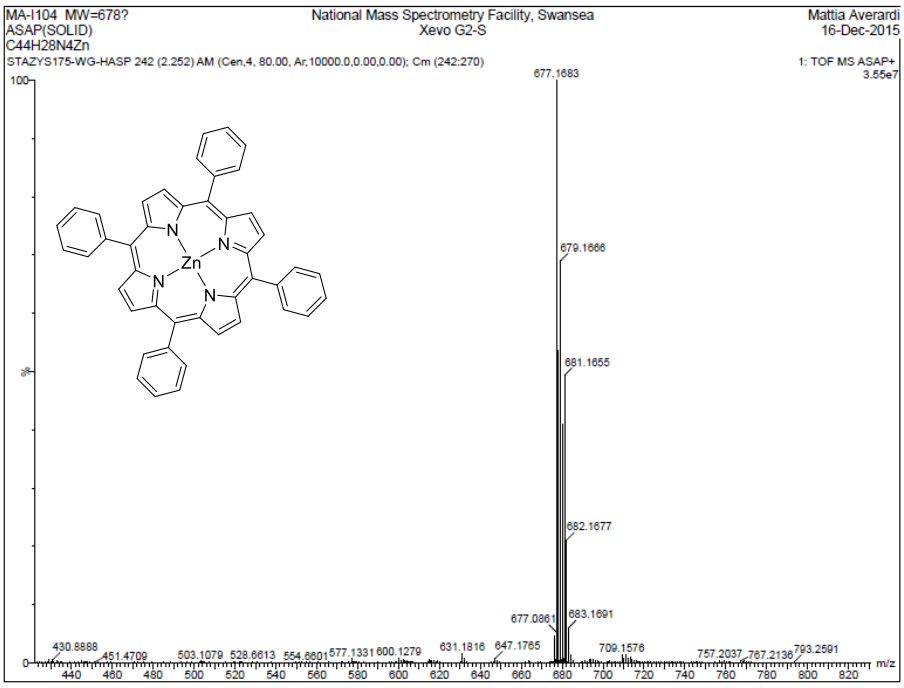


Figure **S8**. HR-MS spectrum of ZnTPP.

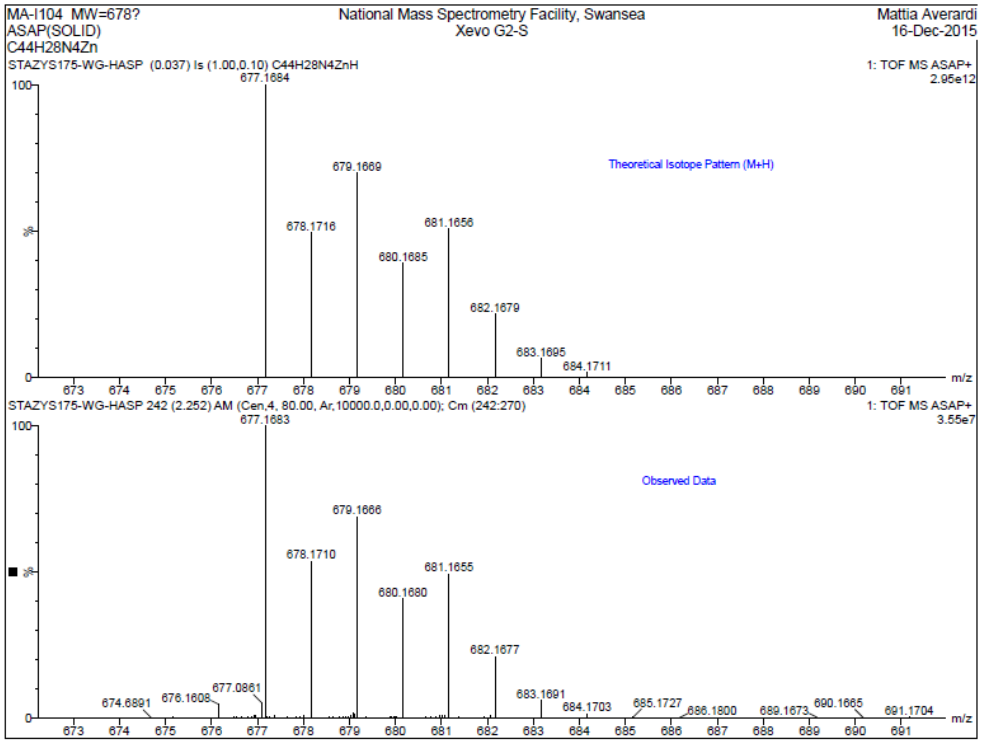


Figure **S9**. Molecular ion of HR-MS spectrum of ZnTPP.

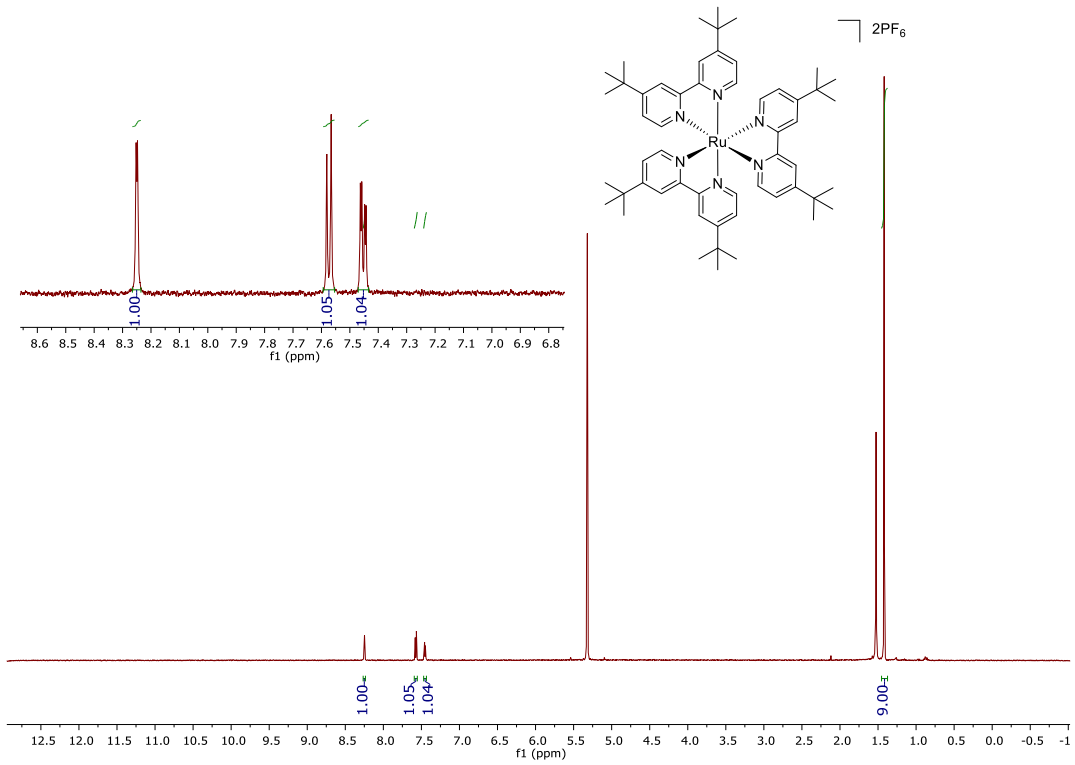


Figure **S10**. $^{1}$H NMR spectrum (400 MHz, $CD_2Cl_2$) of $[Ru(dtBubpy)_3](PF_6)_2$, **2**.

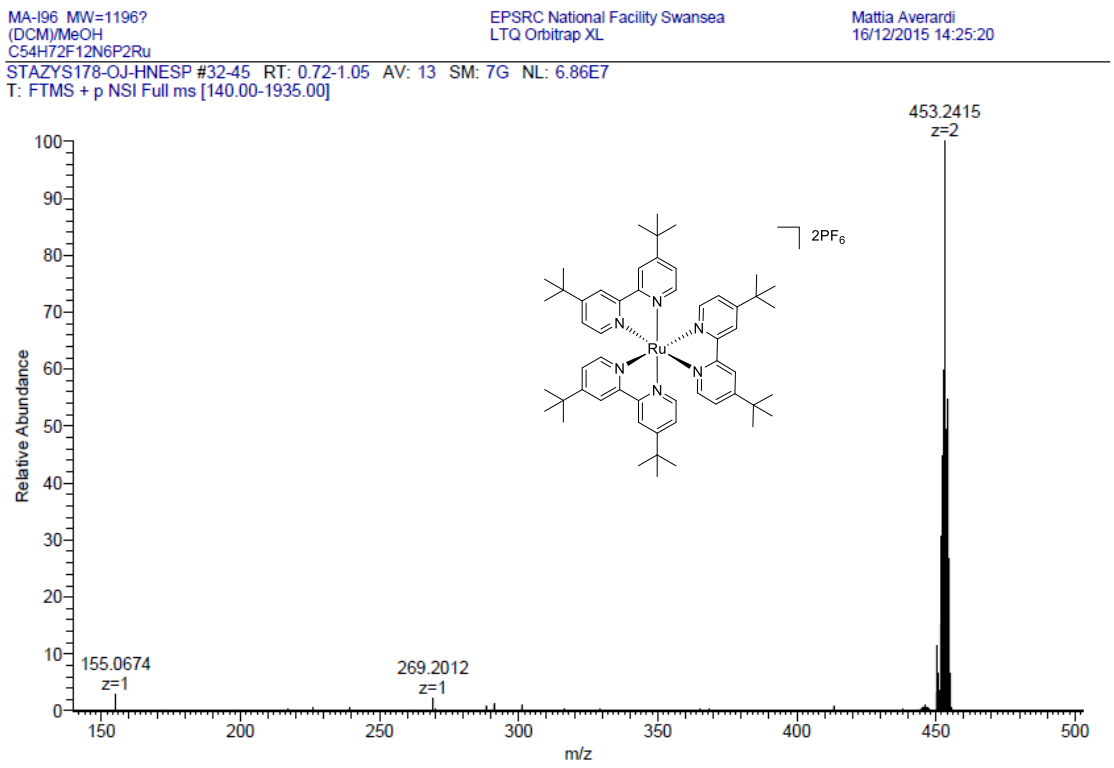


Figure **S11**. HR-MS spectrum of $[Ru(dtBubpy)_3](PF_6)_2$, **2**.

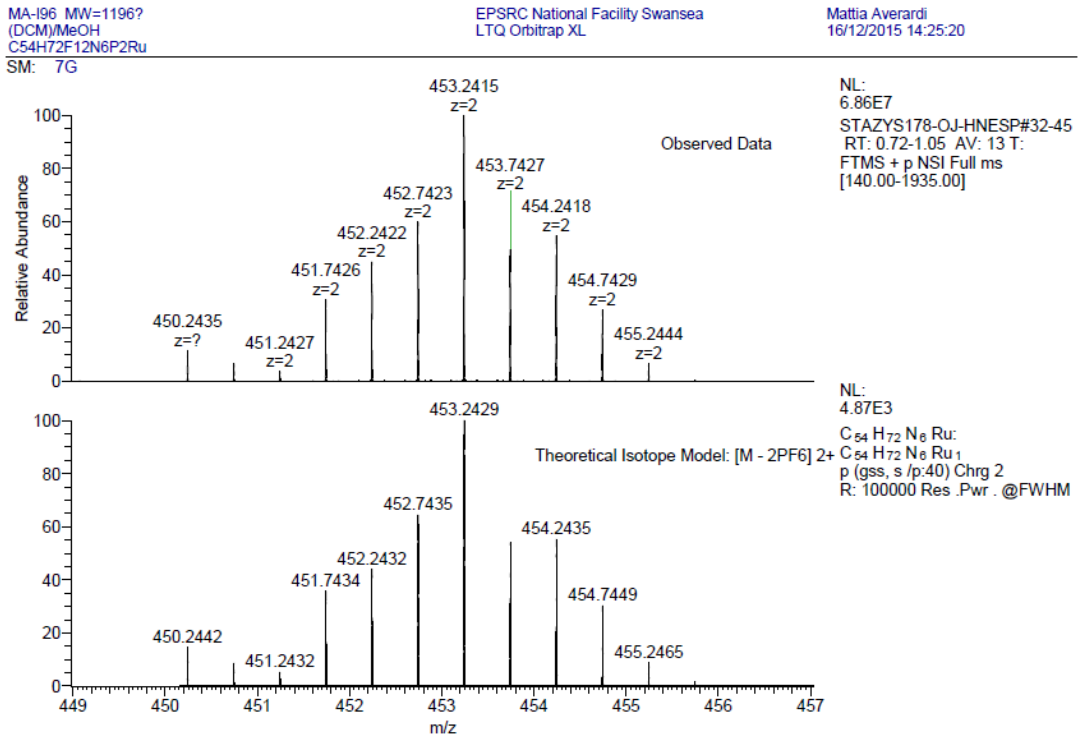

Figure **S12**. Molecular ion of HR-MS of $[Ru(dtBubpy)_3](PF_6)_2$, **2**.

# Determination of association constants in 1a and 1b.

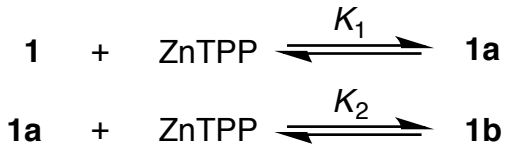


Association constants for the 1:1 complex **1a** and the 1:2 complex **1b** were determined by standard NMR spectroscopic titration methods. Small aliquots of ZnTPP were added to a 3.06 mM solution of **1** in $CD_2Cl_2$ such that the concentration of ZnTPP in the sample carried from 0 mM to 9.44 mM. A $^1$H NMR spectrum was recorded on the solution after each addition and the variation of the chemical shift of $H^a$ in **1** with respect to ZnTPP concentration determined from this data. This data was then fitted to the sequential binding model illustrated in Figure **S14a** using the EQNMR software.[10] The best fit of the binding model to the $^1$H NMR data afforded a value for $K_1$ of 7200 ± 300 $M^{-1}$ and a value for $K_2$ of 2500 ± 350 $M^{-1}$. Speciation data, using two scenarios – [**1**]/[ZnTPP] = 1 and [**1**]/[ZnTPP] = 0.5, were obtained using the parameter scan mode implemented in Gepasi.[11]

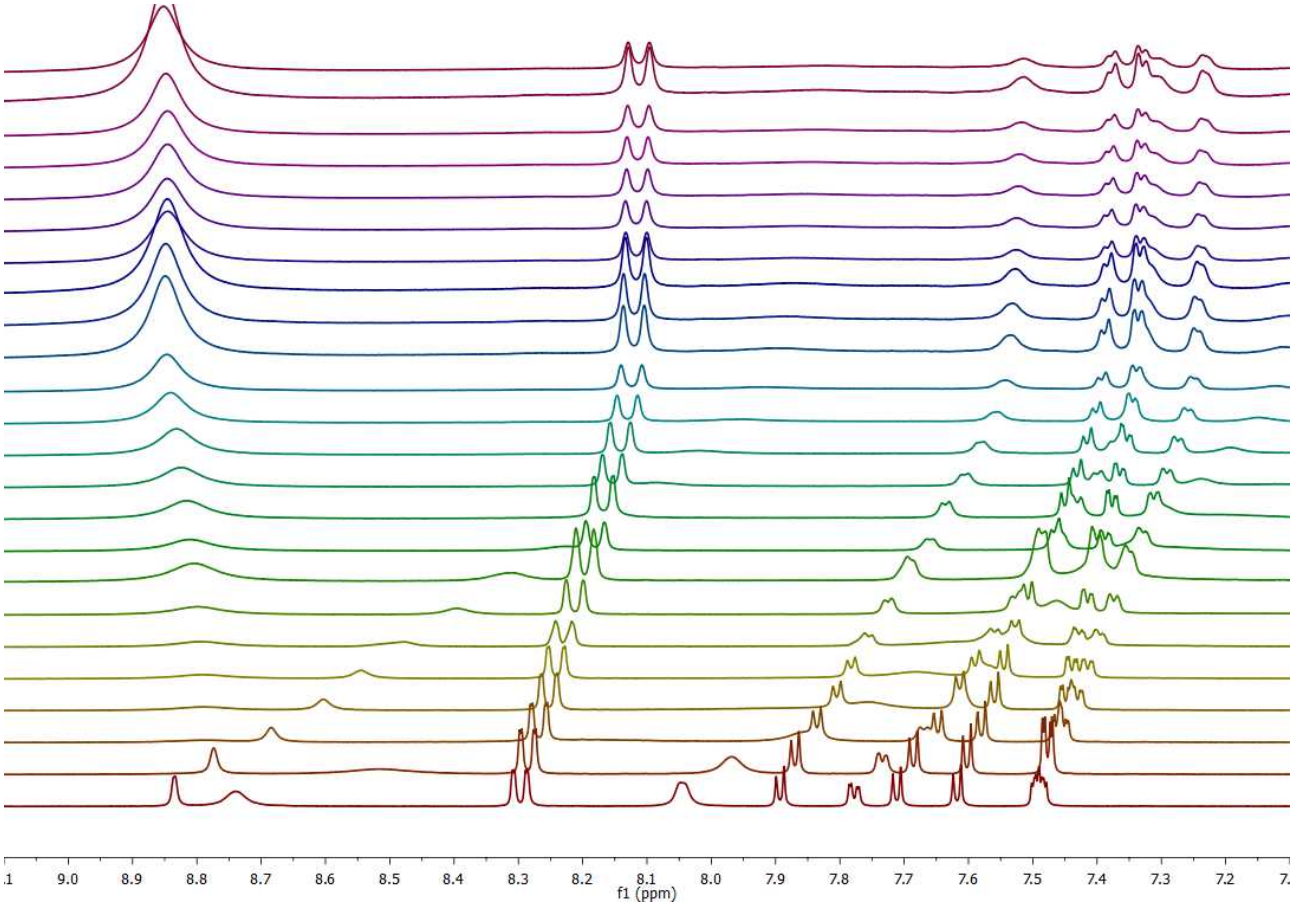


Figure **S13**. $^{1}$H NMR titration experiments, with spectra collected after gradual addition of ZnTPP (from 0.1 equiv. to 2.5 equiv.) to a solution of 3.06 mM of **1**.

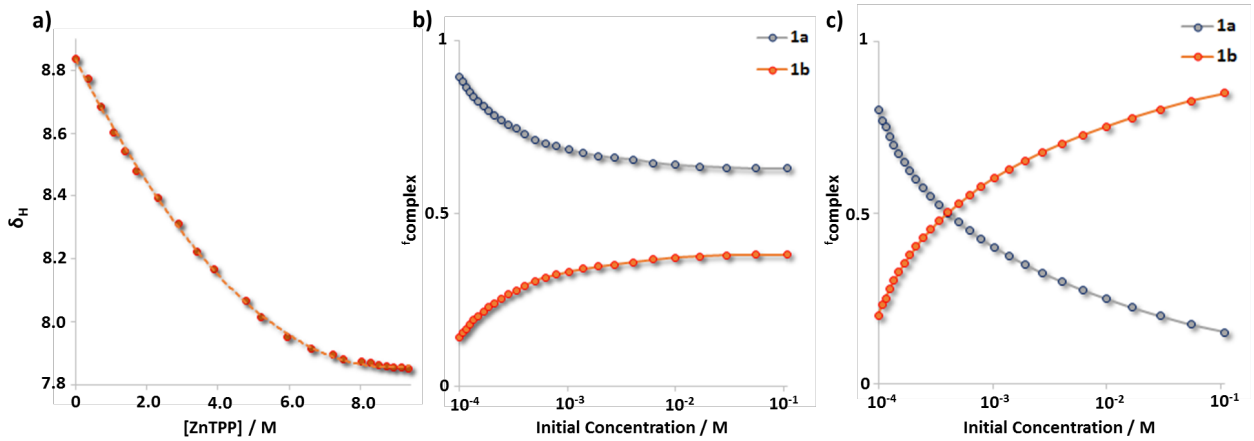


Figure **S14**. **a)** Chemical shift changes observed in the $^{1}$H NMR spectrum of a 3.06 mM solution of **1** in $CD_2Cl_2$ on addition of aliquots of ZnTPP (red points) can be fitted (dotted orange line) to a sequential binding model for the formation of **1a** and **1b**. Fractions of 1:1 complex **1a** (blue lines) and 1:2 complex **1b**

(red lines) present in solution as a function of concentration when **(b)** $[ZnTPP]_{initial}$ = $[\mathbf{1}]_{initial}$ and **(c)** $[ZnTPP]_{initial} = 2 \times [\mathbf{1}]_{initial}$.

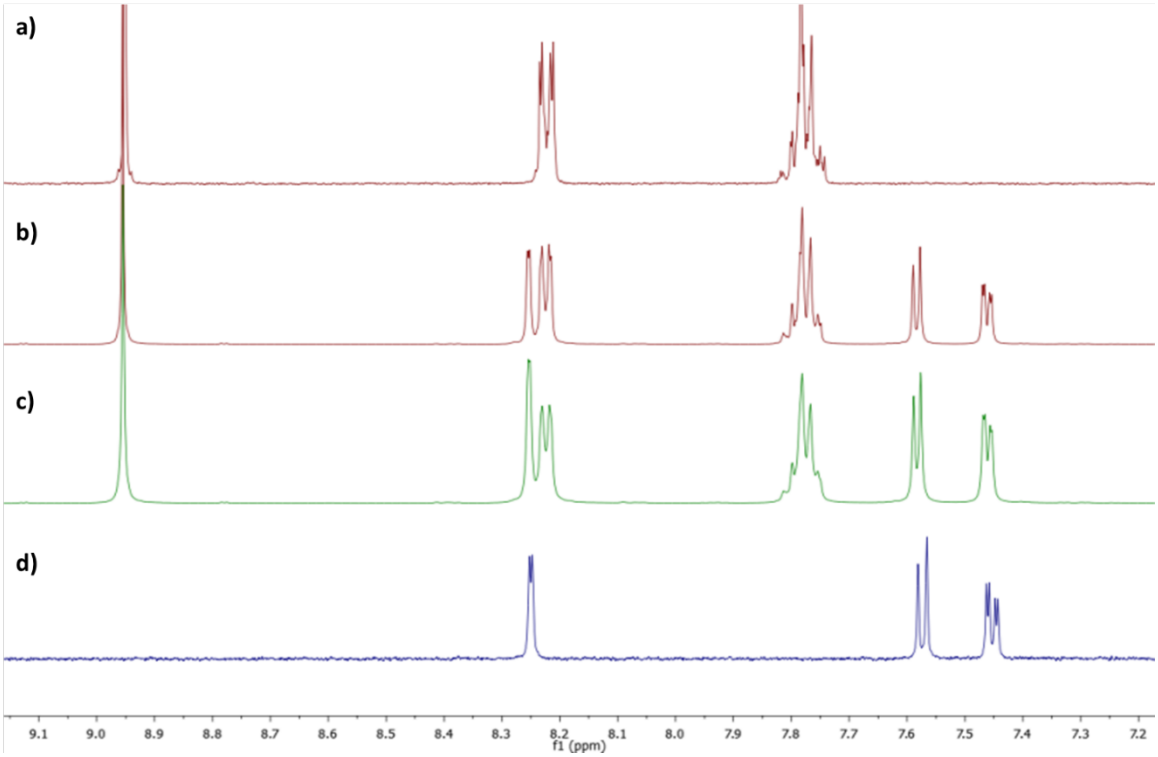


Figure **S15**. Control $^{1}$H NMR spectra ($CD_2Cl_2$, 500 MHz, 298 K) of **a**) ZnTPP, **b**) a mixture of complex **2** and 1 equivalent of ZnTPP, c) a mixture of **2** and 2 equivalents of ZnTPP and **d)** complex **2**.

# Supplementary Optoelectronic Characterization.

## UV-Vis spectroscopy.

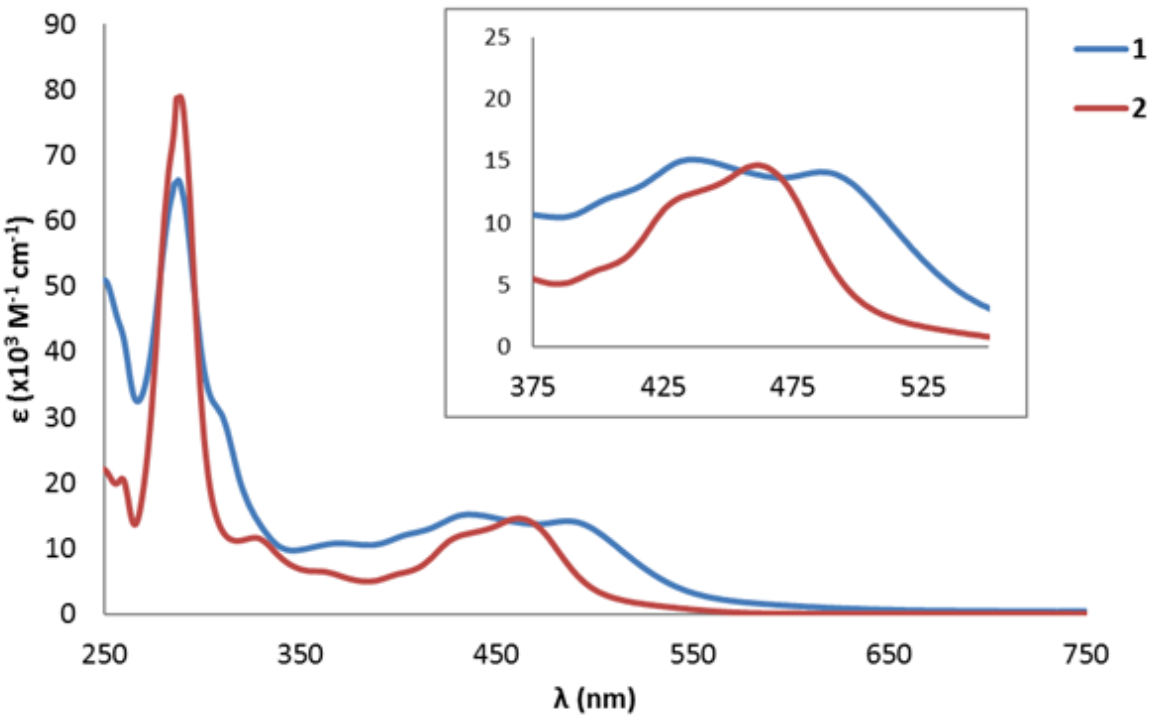


Figure **S16**. UV-Vis spectra of $[Ru(dtBubpy)_2(qpy)]2PF_6$ (**1,** in blue), $[Ru(dtBubpy)_3]_2PF_6$ (**2,** in red) collected in $CD_2Cl_2$ at 298 K with a concentration on the order of $10^{-6}$M.

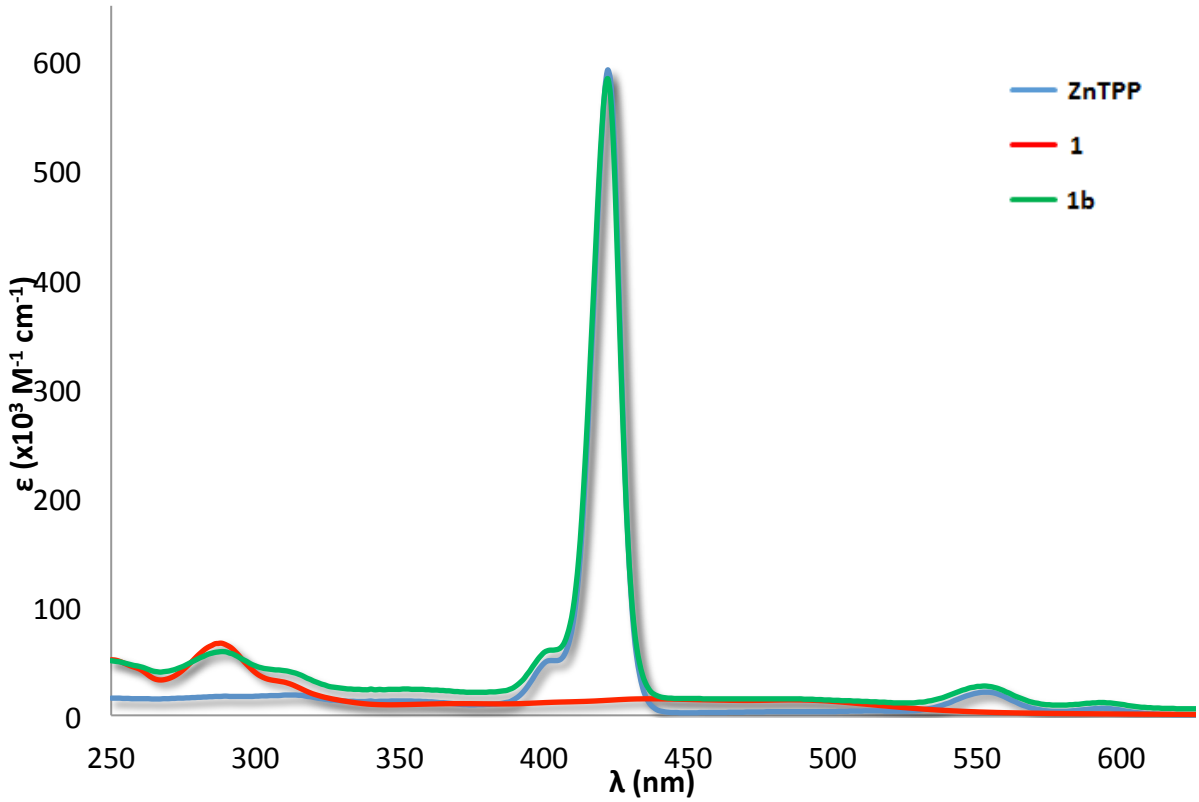

Figure **S17**. UV-Vis spectra of ZnTPP, (in light-blue), [Ru(dtBubpy)$_2$(qpy)]2PF$_6$ (**1,** in red) and assembly **1b** (in green) collected in $CD_2Cl_2$ at 298 K with a concentration on the order of $10^{-6}$M.

| Compound | $l_{max}$(vis)[a] [ε(×$10^3$ $M^{-1}$ $cm^{-1}$)][b] |
|---|---|
| **ZnTPP** | 285 [43.0], 399 [48.5], 422 [598], 480 [1.9], 513 [3.4], 553 [23.0], 595 [5.7] |
| **1** | 289 [65.5], 311 [29.6], 373 [10.7], 437 [15.1], 492 [13.9] |
| **2** | 290 [78.0], 331 [11.2], 369 [6.0], 429 [11.7], 469 [13.7] |
| **1b** | 290 [58.0], 311 [39.2], 403 [59.7], 422 [593.2], 554 [26.5], 596 [11.0] |

Table **S1**. [a] UV-Vis absorption in DCM with a concentration in the order of $10^{-6}$ M collected at 298 K. [b]concentration-independent extinction coefficients.

# Cyclic Voltammetry and Differential Pulse Voltammetry.

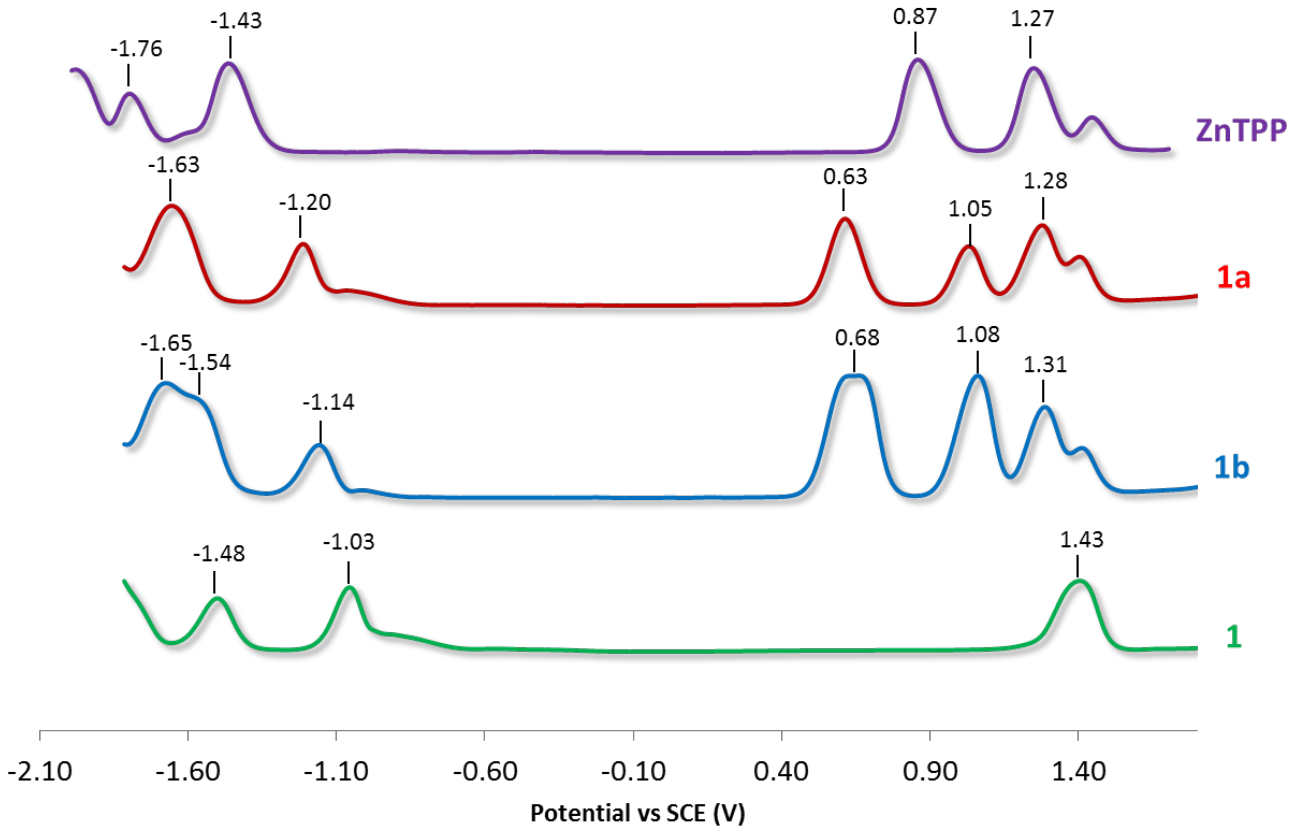


Figure **S18**. Differential Pulse Voltammograms for complex **1** (green line), assemblies **1a** (red line) and **1b** (light-blue line) and ZnTPP (purple line) recorded at 298 K in deareated DCM solution containing *n*-$NBu_4PF_6$ as the supporting electrolyte and using $Fc/Fc^+$ as an internal standard ($Fc/Fc^+$ = 0.46 V in DCM with respect to SCE).

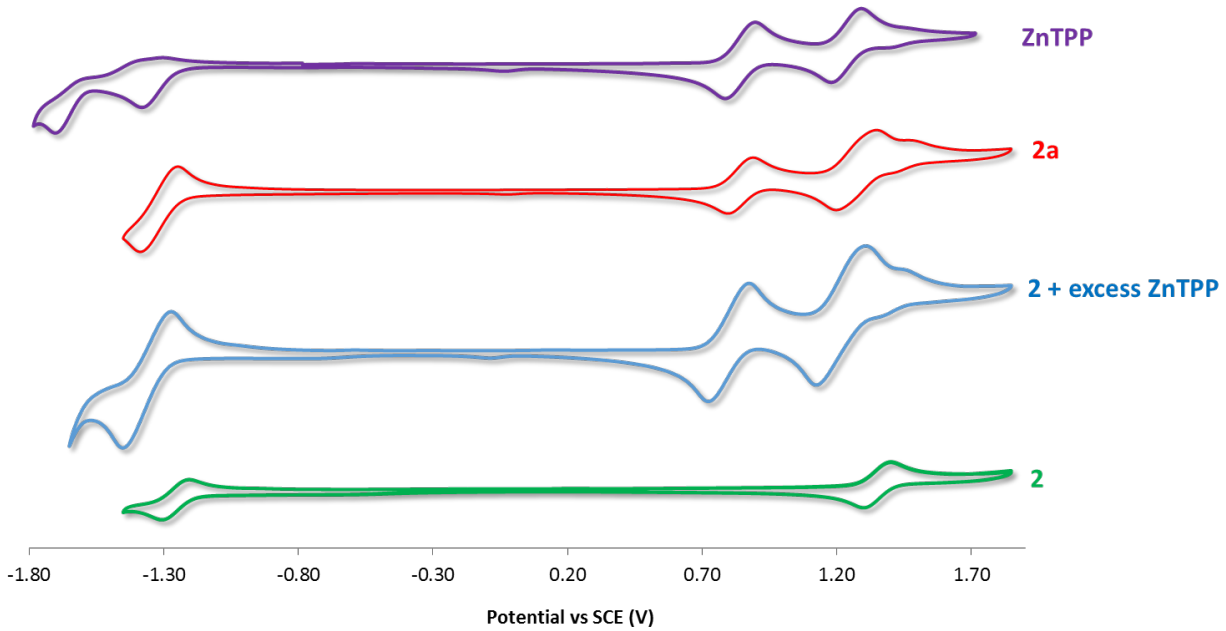

Figure **S19**. Cyclic Voltammograms for complex **2** (green line), "non-assemblies **2a**" (red line), **2** with an excess of ZnTPP (light-blue line) and ZnTPP (purple line) recorded at 298 K in deareated DCM solution containing *n*-$NBu_4PF_6$ as the supporting electrolyte and using $Fc/Fc^+$ as an internal standard ($Fc/Fc^+$ = 0.46 V in DCM with respect to SCE).

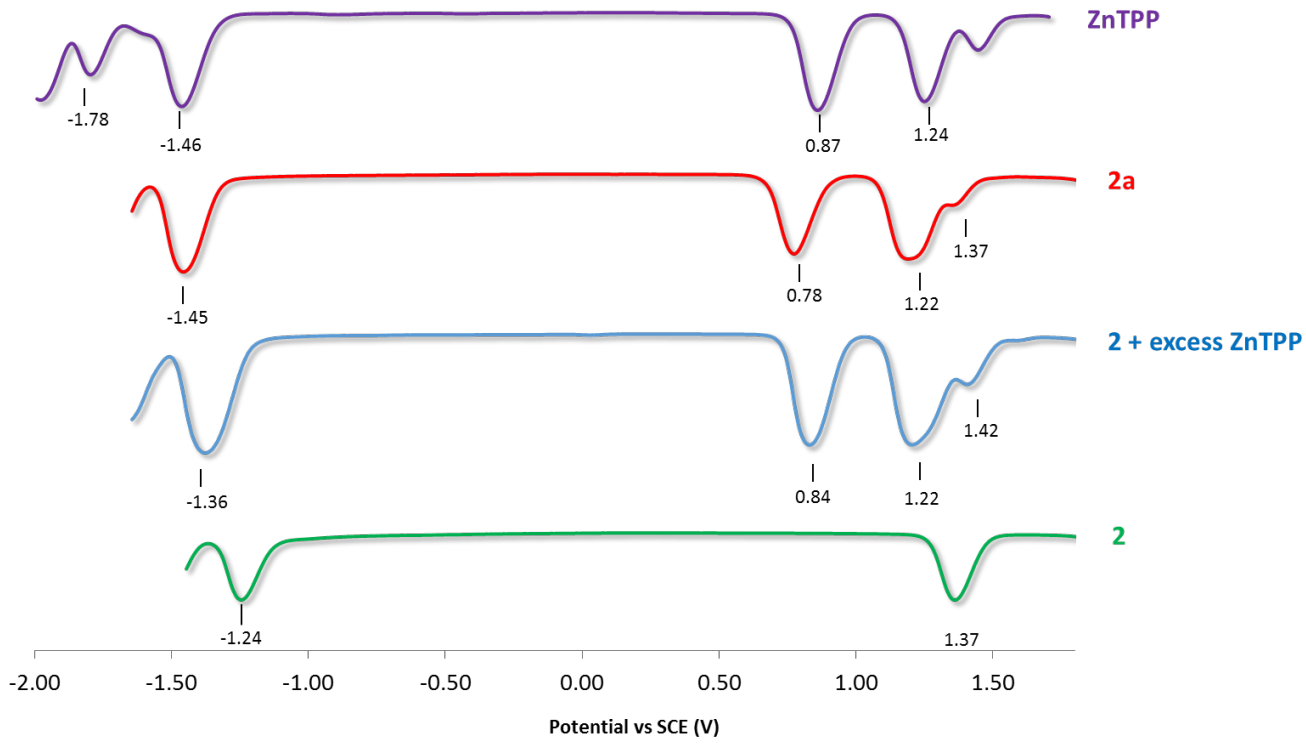


Figure **S20**. Differential Pulse Voltammograms for complex **2** (green line), "non-assemblies **2a**" (red line), **2** with an excess of ZnTPP (light-blue line) and ZnTPP (purple line) recorded at 298 K in deareated DCM solution containing *n*-$NBu_4PF_6$ as the supporting electrolyte and using $Fc/Fc^+$ as an internal standard ($Fc/Fc^+$ = 0.46 V in DCM with respect to SCE).

# Emission studies.

| | $\lambda_{em}$ (nm) [a,b] | | FΦ (%) [a,c] | |
|---|---|---|---|---|
| | λexc = 420 nm | λexc = 555 nm | λexc = 420 nm [c] | λexc = 555 nm [c] |
| **ZnTPP** | 605 [0.6], 651 [1], 716 [0.04] | 605 [0.6], 651 [1], 716 [0.04] | 3.7 | 0.8 |

| | | | | |
|---|---|---|---|---|
| **1** | 672 [1] | 672 [1] | - | 7.3 |
| **1a** | 601 [0.09], 655 [1] | 601 [0.09], 655 [1] | < 1[d] | < 1[d] |
| **1b** | 603 [0.19], 655 [1] | 603 [0.19], 655 [1] | < 1[d] | <1[d] |
| **2** | 615 [1] | 615 [1] | - | 9.1 |
| **2a** | 599 [0.05], 655 [1] | 599 [0.05], 655 [1] | 1.4 | < 1[d] |

Table **S2**. [a] Measurements in deaerated DCM at 298 K at *ca*. $10^{-5}$ M. [b] Relative intensity of principal emission peaks listed in [ ]. [c] Using $[Ru(bpy)_3]Cl_2$ as the standard ($\Phi_{PL}$ = 4% in aerated $H_2O$ at 298 K). [d] Estimated from the reduction of the emission counting compared to neat ZnTPP.

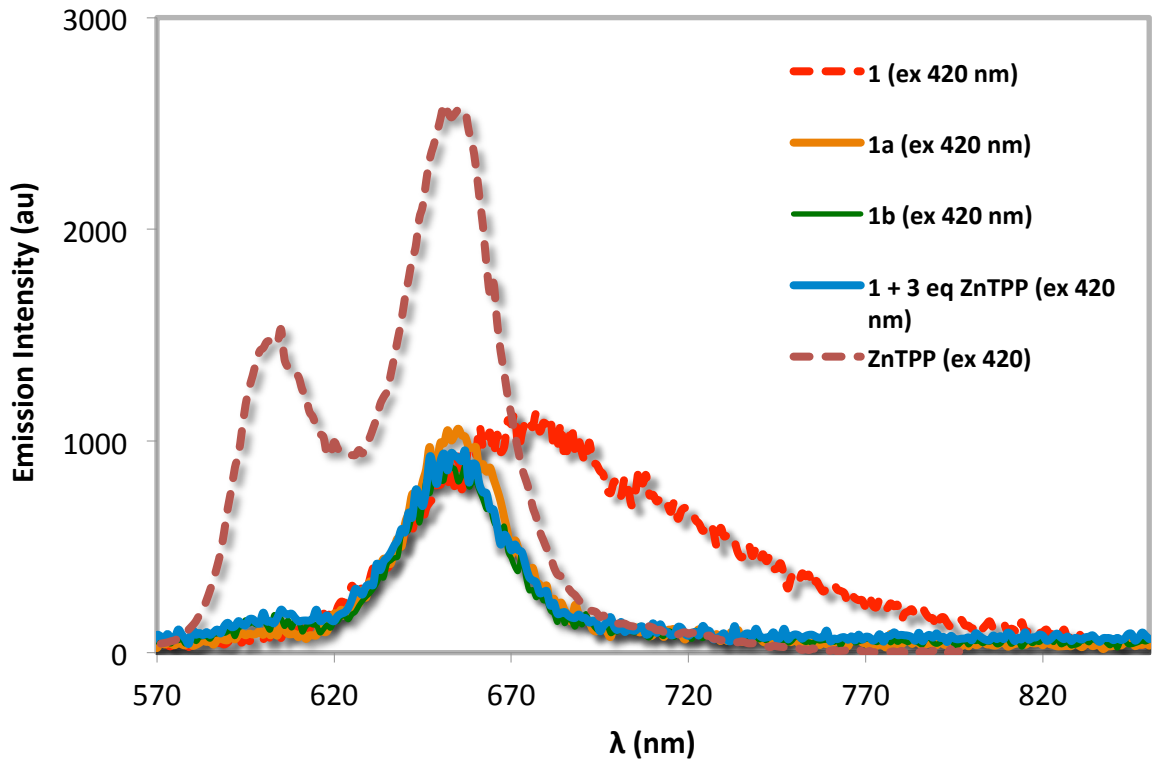


Figure **S21**. Luminescence spectra of **1** (dotted red line), **1a** (solid orange line), **1b** (solid green line), 1 with an excess of ZnTPP (solid blue line) and ZnTPP (dotted brown line) recorded in degassed DCM at 298 K ($\lambda_{ex}$ = 420 nm) with a concentration in the order of $3 \times 10^{-4}$ M.

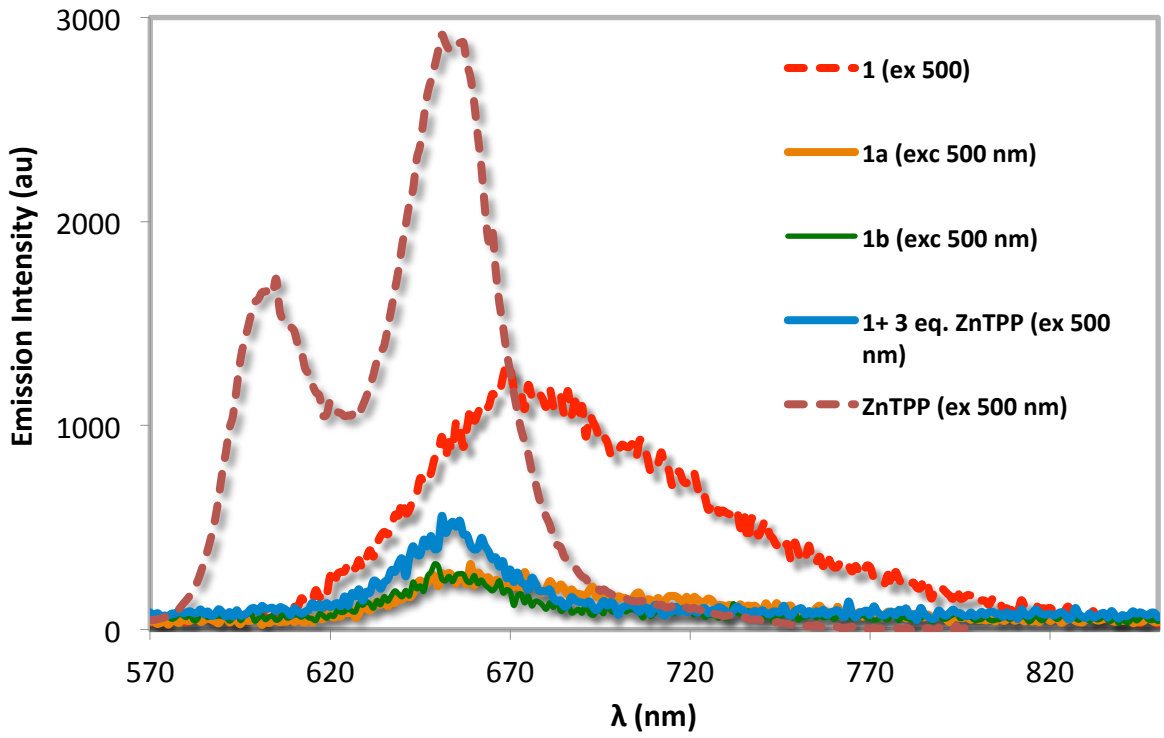


Figure **S22**. Luminescence spectra of **1** (dotted red line), **1a** (solid orange line), **1b** (solid green line), 1 with an excess of ZnTPP (solid blue line) and ZnTPP (dotted brown line) recorded in degassed DCM at 298 K ($\lambda_{ex}$ = 500 nm) with a concentration in the order of $3 \times 10^{-4}$ M.

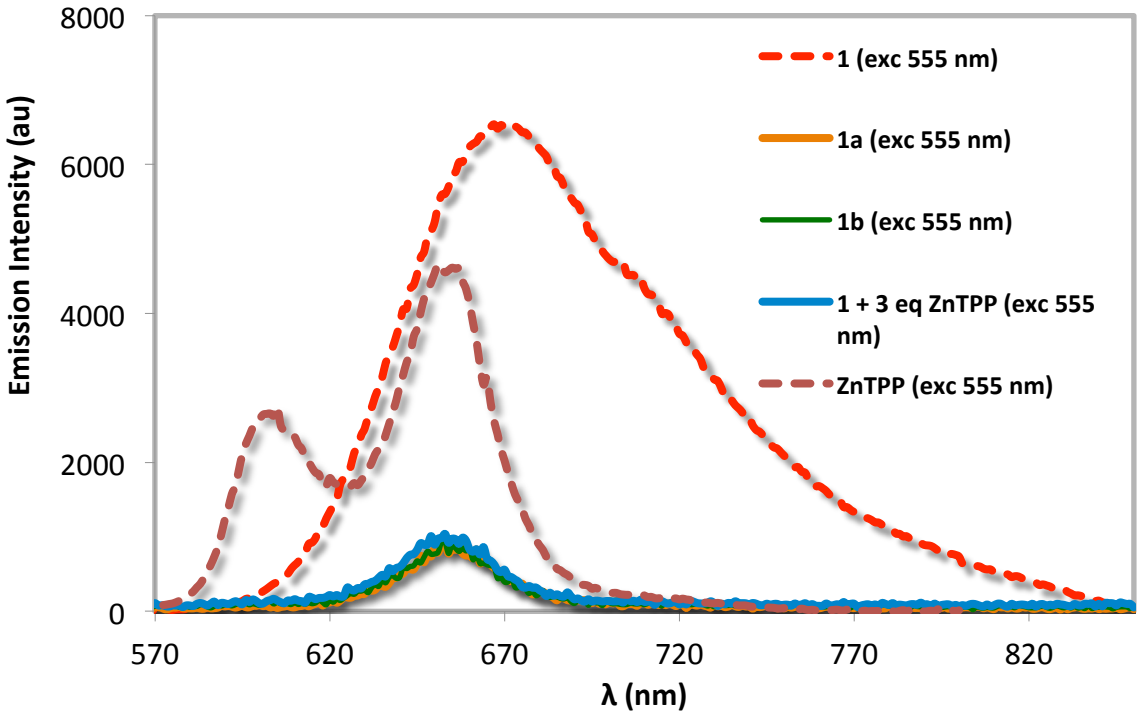

Figure **S23**. Luminescence spectra of **1** (dotted red line), **1a** (solid orange line), **1b** (solid green line), 1 with an excess of ZnTPP (solid blue line) and ZnTPP (dotted brown line) recorded in degassed DCM at 298 K ($\lambda_{ex}$ = 550 nm) with a concentration in the order of $3 \times 10^{-4}$ M.

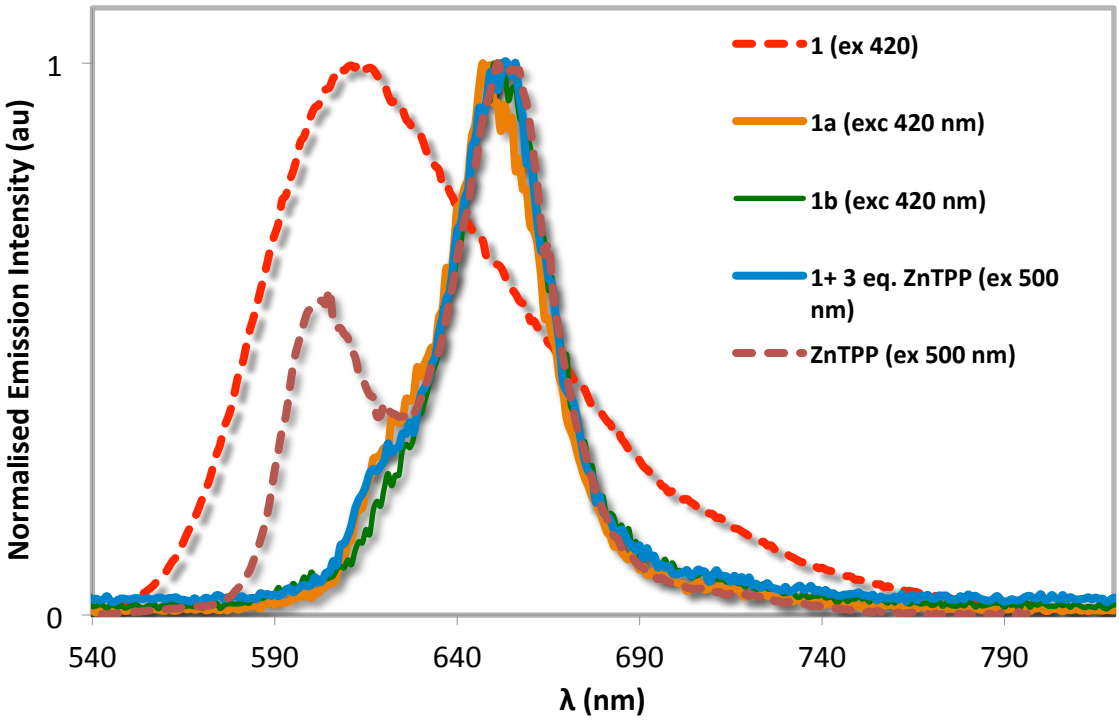


Figure **S24**. Luminescence spectra of **2** (dotted red line), **2** with 1 equiv. of ZnTPP (solid orange line), **2** with 2 equiv. of ZnTPP (solid green line), **2** with 3 equiv. of ZnTPP (solid blue line) and ZnTPP (dotted brown line) recorded in degassed DCM at 298 K ($\lambda_{ex}$ = 500 nm) with a concentration in the order of $3 \times 10^{-4}$ M.

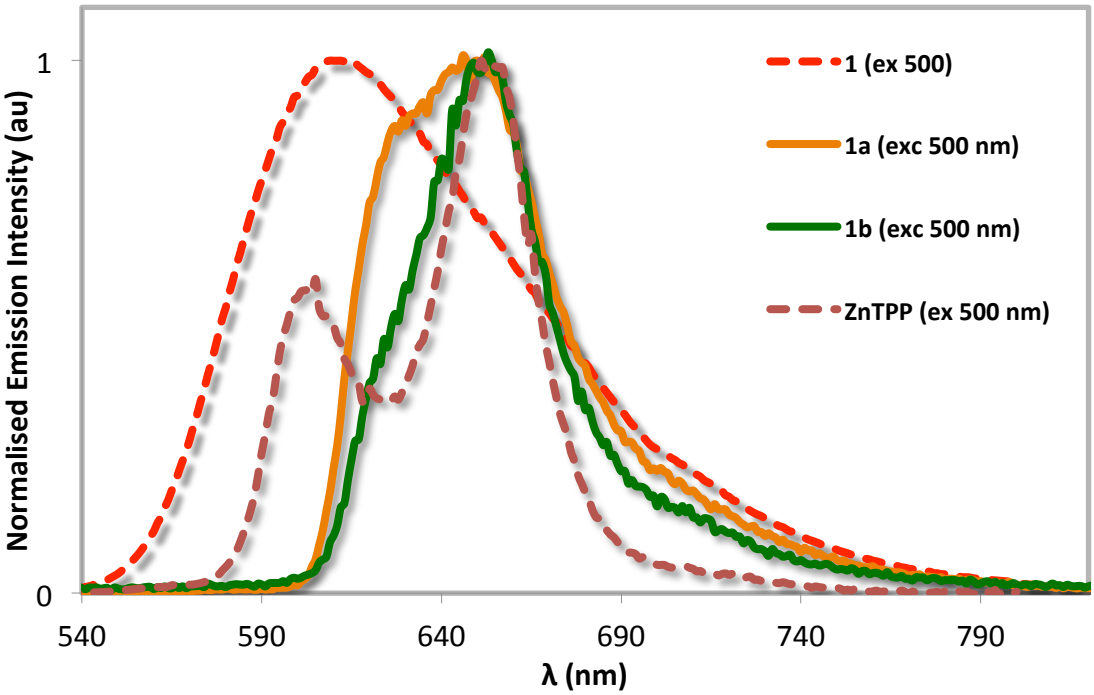


Figure **S25**. Luminescence spectra of **2** (dotted red line), **2** with 1 equiv. of ZnTPP (solid orange line), **2** with 2 equiv. of ZnTPP (solid green line) and ZnTPP (dotted brown line) recorded in degassed DCM at 298 K ($\lambda_{ex}$ = 500 nm) with a concentration in the order of $3 \times 10^{-4}$ M.

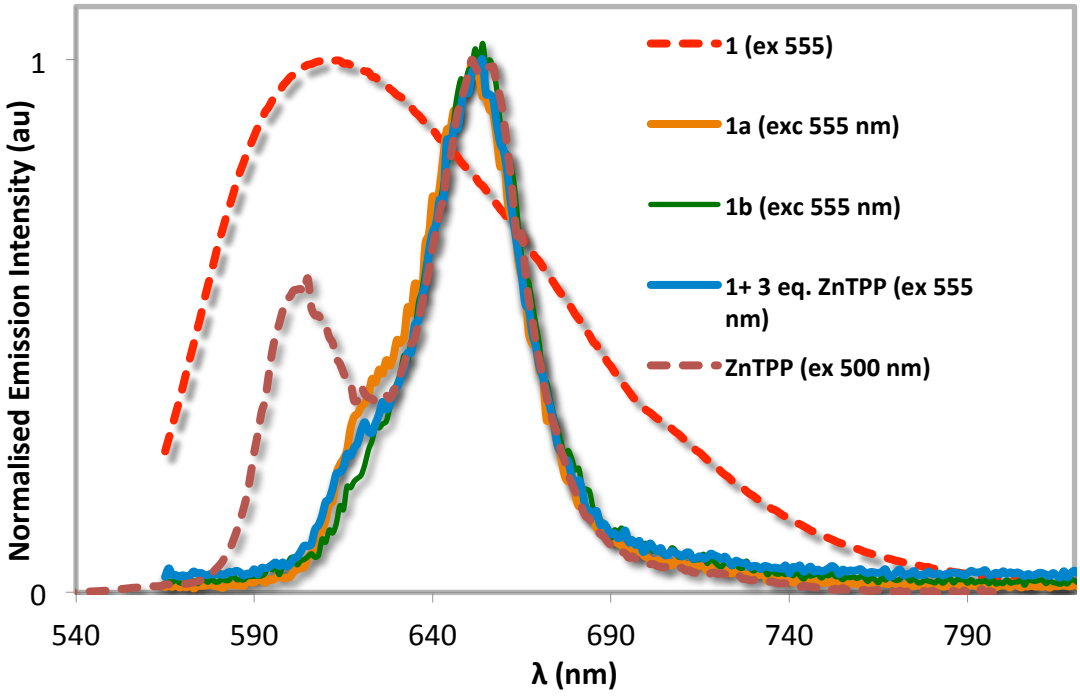

Figure **S26**. Luminescence spectra of **2** (dotted red line), **2** with 1 equiv. of ZnTPP (solid orange line), **2** with 2 equiv. of ZnTPP (solid green line), **2** with 3 equiv. of ZnTPP (solid blue line) and ZnTPP (dotted brown line) recorded in degassed DCM at 298 K ($\lambda_{ex}$ = 550 nm) with a concentration in the order of $3 \times 10^{-4}$ M.

# Computational details.

All calculations use density functional theory (DFT). The geometries of the singlet ground-state ($S_0$) and the lowest triplet excited-state ($T_1$) were optimized for complex **1** and the assembly **1a** using the hybrid exchange-correlation functional B3LYP[12] in combination with the def2-SVP atomic basis set under the resolution of the identity (RI) approximation. Scalar relativistic effects were included for the Ru atom by using the ECP-28-mwb Stuttgart/Dresden pseudopotential.[13] The nature of the stationary points was confirmed by computing the Hessian at the same level of theory. Gas-phase TD-B3LYP vertical singlet energies were obtained at the $S_0$ geometry using the def2-SVP atomic basis set. Optimizations and TD-DFT calculations were carried out with the Turbomole 6.6 program package.[14]

Table **S3.** Main Vertical (at $S_0$ geometry) Singlet Electronic Transition Energies (in eV) and Oscillator strengths (in Parentheses) of 1 at the TD-B3LYP/def2-SVP Level of Theory.

| | States | Energy (*f*) | Character |
|---|---|---|---|
| **1** | $S_4$ | 2.69 (0.036) | $^1$MLCT ($d_{Ru} \rightarrow \pi^*_{dtBubpy+qpy}$) |
| | $S_7$ | 2.83 (0.164) | $^1$MLCT ($d_{Ru} \rightarrow \pi^*_{dtBubpy+qpy}$) |
| | $S_8$ | 2.86 (0.107) | $^1$MLCT($d_{Ru} \rightarrow \pi^*_{dtBubpy+qpy}$) |
| | $S_{41}$ | 3.93 (0.103) | $^1$LC ($\pi_{qpy} \rightarrow \pi^*_{dtBubpy+qpy}$) |

# References.


(1). N. A. F. Al-Rawashdeh, S. Chatterjee, J. A. Krause and W. B. Connick, *Inorg. Chem.*, 2014, **53**, 294-307.
(2). N. Zabarska, J. G. Vos and S. Rau, *Polyhedron*, 2015, **102**, 173-175.
(3). D. Rota Martir, G. J. Hedley, D. B. Cordes, A. M. Z. Slawin, D. Escudero, D. Jacquemin, T. Kosikova, D. Philp, D. M. Dawson, S. E. Ashbrook, I. D. W. Samuel and E. Zysman-Colman, *Dalton Trans.*, 2016, **45**, 17195-17205.
(4). B. J. Coe, E. C. Harper, M. Helliwell and Y. T. Ta, *Polyhedron*, 2011, **30**, 1830-1841.
(5). H. Huang, B. Yu, P. Zhang, J. Huang, Y. Chen, G. Gasser, L. Ji and H. Chao, *Angew. Chem. Int. Ed.*, 2015, **54**, 14049-14052.
(6). M. Schwalbe, B. Schäfer, H. Görls, S. Rau, S. Tschierlei, M. Schmitt, J. Popp, G. Vaughan, W. Henry and J. G. Vos, *Eur. J. Inorg. Chem.*, 2008, **2008**, 3310-3319.
(7). G. A. Crosby and J. N. Demas, *J. Phys. Chem.*, 1971, **75**, 991-1024.
(8). (a) K. Suzuki, A. Kobayashi, S. Kaneko, K. Takehira, T. Yoshihara, H. Ishida, Y. Shiina, S. Oishi and S. Tobita, *Phys Chem Chem Phys*, 2009, **11**, 9850-9860; (b) A. M. Brouwer, *Pure Appl. Chem.*, 2011, **83**, 2213-2228.
(9). N. G. Connelly and W. E. Geiger, *Chem. Rev.*, 1996, **96**, 877-910.
(10). M. J. Hynes, *J. Chem. Soc., Dalton Trans.*, 1993, 311-312.
(11). (a) P. Mendes, *Computer applications in the biosciences : CABIOS*, 1993, **9**, 563-571; (b) P. Mendes and D. Kell, *Bioinformatics*, 1998, **14**, 869-883.
(12). (a) A. D. Becke, *J. Chem. Phys.*, 1993, **98**, 5648-5652; (b) C. Lee, W. Yang and R. G. Parr, *Phys. Rev. B*, 1988, **37**, 785-789.
(13). D. Andrae, U. Häußermann, M. Dolg, H. Stoll and H. Preuß, *Theoretica chimica acta*, **77**, 123-141.
(14). *TURBOMOLE V6.6; a development of University of Karlsruhe and Forschungszentrum Karlsruhe GmbH, 1989–2007; TURBOMOLEGmbH, since2007. Available from* http://www.turbomole.com., 2014.